Environmental Science & Technology

pubs.acs.org/est

Article

Characterization of Annual Average Traffic-Related Air Pollution Concentrations in the Greater Seattle Area from a Year-Long Mobile Monitoring Campaign

Magali N. Blanco,* Amanda Gassett, Timothy Gould, Annie Doubleday, David L. Slager, Elena Austin, Edmund Seto, Timothy V. Larson, Julian D. Marshall, and Lianne Sheppard

Cite This: *Environ. Sci. Technol.* 2022, 56, 11460−11472

Read Online

ACCESS | Metrics & More | Article Recommendations | Supporting Information

ABSTRACT: Growing evidence links traffic-related air pollution (TRAP) to adverse health effects. We designed an innovative and extensive mobile monitoring campaign to characterize TRAP exposure levels for the Adult Changes in Thought (ACT) study, a Seattle-based cohort. The campaign measured particle number concentration (PNC) to capture ultrafine particles (UFP), black carbon (BC), nitrogen dioxide (NO_2), fine particulate matter ($PM_{2.5}$), and carbon dioxide (CO_2) at 309 roadside sites within a large, 1200 land km^2 (463 mi^2) area representative of the cohort. We collected about 29 two-minute measurements at each site during all seasons, days of the week, and most times of the day over a 1-year period. Validation showed good agreement between our BC, NO_2, and $PM_{2.5}$ measurements and monitoring agency sites (R^2 = 0.68−0.73). Universal kriging−partial least squares models of annual average pollutant concentrations had cross-validated mean square error-based R^2 (and root mean square error) values of 0.77 (1177 pt/cm^3) for PNC, 0.60 (102 ng/m^3) for BC, 0.77 (1.3 ppb) for NO_2, 0.70 (0.3 μg/m^3) for $PM_{2.5}$, and 0.51 (4.2 ppm) for CO_2. Overall, we found that the design of this extensive campaign captured the spatial pollutant variations well and these were explained by sensible land use features, including those related to traffic.

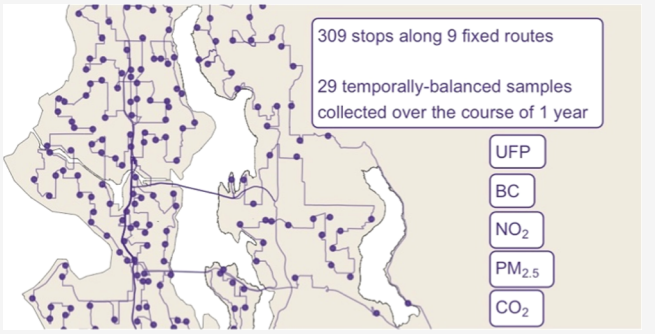

KEYWORDS: *mobile monitoring, air pollution, particle number count (PNC), ultrafine particles (UFP), black carbon (BC), nitrogen dioxide (NO_2), exposure assessment, epidemiology*

1. INTRODUCTION

An extensive body of evidence has linked air pollution to adverse health effects including respiratory, cardiovascular, and mortality outcomes.[1] Recent evidence has begun to link traffic-related air pollution (TRAP) exposure to cognitive function among various populations, including the elderly.[2−6] While TRAP is a complex mixture that varies over time and space, pollutants include ultrafine particles (UFPs; typically defined as particles with aerodynamic diameter ≤ 100 nm), black carbon (BC), oxides of nitrogen including nitrogen dioxide (NO_2), and carbon dioxide (CO_2).[7] In particular, UFPs have increasingly been associated with health outcomes, including elevated levels of neurotoxicity and systemic inflammation when compared to larger particles.[8−14]

To date, however, much of the epidemiology air pollution research has been limited to the federally defined criteria air pollutants, monitored nationwide through the EPA's regulatory Air Quality System (AQS) monitoring network. This network is supported by local monitoring agencies and has measured criteria pollutant levels throughout the US since the 1990s, although none specifically include UFPs.[15] Furthermore, this network is spatially sparse and thus fails to capture the spatial variability of more quickly decaying pollutants, including many TRAPs.[16] The Seattle Census Urbanized Area, for example, averages about 1 AQS monitor every 174 km^2 (~14 active monitors within about 2,440 km^2), most of which measure the mass concentration of fine particulate matter with a diameter of less than 2.5 μm ($PM_{2.5}$) and BC.[17,18]

Mobile monitoring campaigns for assessing air pollution exposure have been used since at least the 1970s and have become increasingly common in recent years in an effort to address the limitations of traditional fixed-site monitoring approaches.[19−26] Typically, a vehicle is equipped with air monitors capable of measuring pollutants with high temporal resolution. The platform is used to repeatedly collect short-

Received: February 11, 2022
Revised: July 22, 2022
Accepted: July 25, 2022
Published: August 2, 2022

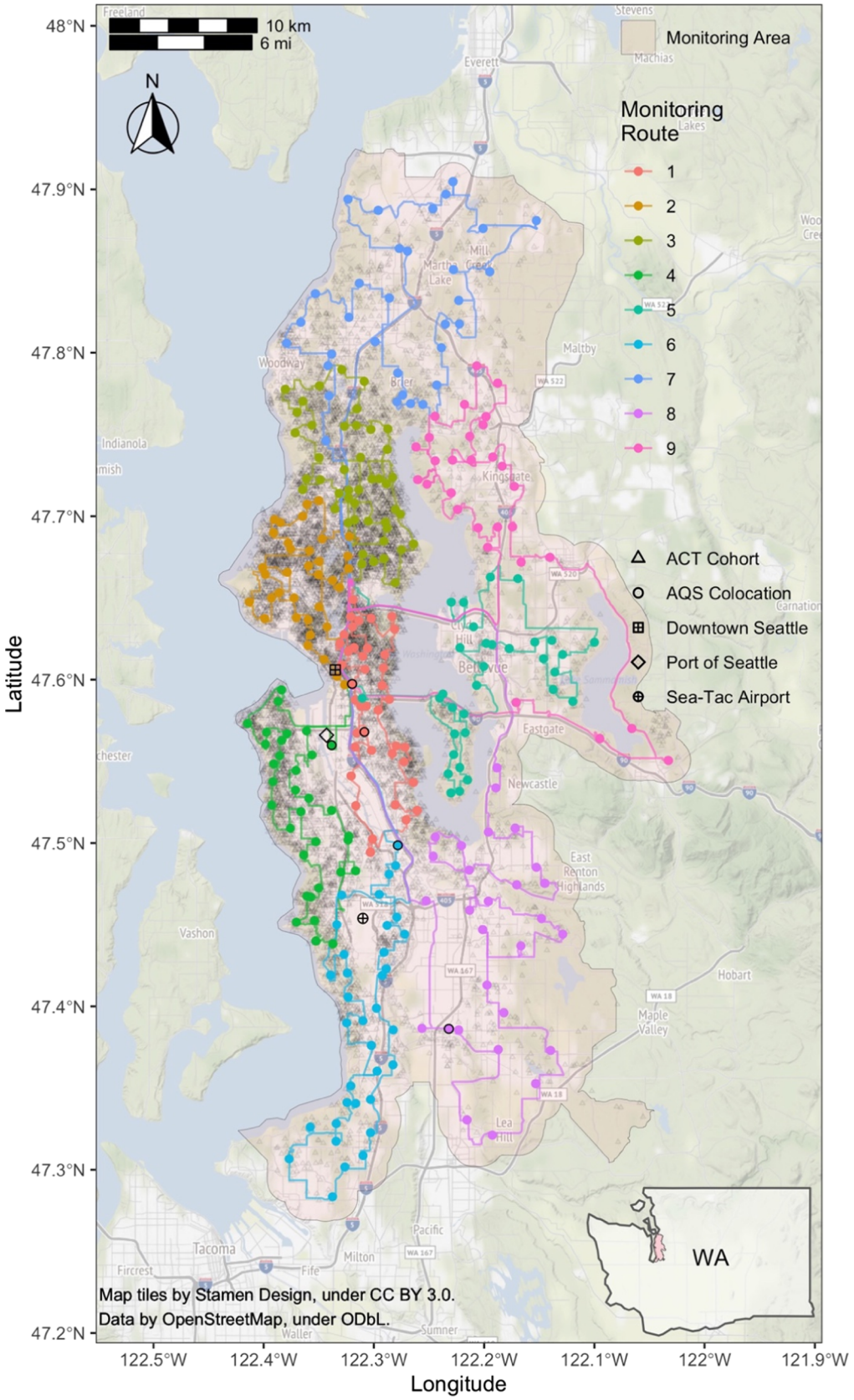

Figure 1. Mobile monitoring routes (n = 309 sites along nine routes) and jittered ACT cohort locations (n = 10,330 unique sites). The inset map shows the monitoring area within the Washington (WA) state.

term samples at predefined sites. Past work has shown that repeated short-term air pollution samples can be used to calculate unbiased long-term averages, thus reducing the need for continuous fixed-site monitoring.[19,20,27] Because the

https://doi.org/10.1021/acs.est.2c01077
Environ. Sci. Technol. 2022, 56, 11460−11472

sampling duration at individual sites can be quite short, campaigns can increase their spatial coverage with a single platform, thus making this approach more time- and cost-efficient than traditional fixed-site monitoring.

Still, the designs of past mobile monitoring campaigns have arguably limited their epidemiologic application. Importantly, most campaigns have been sampled during limited time periods, for example, weekday business hours during one to three seasons.[21,28−30] We previously showed that these limited sampling campaigns likely result in biased long-term exposure estimates because they do not capture the high temporal variability of many TRAPs and that the exact degree of bias varies (is not consistent) across sites.[27] Heterogeneous diurnal patterns in TRAP exposures have been recently shown to occur on a fine spatial scale, motivating the need for a balanced sampling design to reduce biases in the annual average estimates.[31] Additionally, many campaigns have sampled along nonresidential areas such as highways and industrial areas where air pollution levels may be much higher than the levels that most people are exposed to. Most have also collected nonstationary (mobile) on-road samples rather than stationary samples along the side of the road closer to participants' residences. While nonstationary designs increase spatial coverage, further work is needed to demonstrate whether these are representative of residential human exposure levels.[21,32] The additional bias that likely results from these limited sampling schemes is unclear.

To address the limitations of past campaigns, we designed an extensive, multipollutant mobile monitoring campaign to characterize TRAP exposure levels for the Adult Changes in Thought (ACT) study cohort. ACT is a long-standing, prospective cohort study that has been investigating aging and brain health in the greater Seattle area since 1995.[33] The campaign measured TRAP at 309 stationary roadside sites representative of the cohort in a temporally balanced approach throughout the course of a year. The goal of this paper is to describe the design and implementation of a novel mobile monitoring methodology explicitly developed to produce relatively unbiased exposure predictions of annual average exposures to TRAP for the ACT cohort. To the best of our knowledge, this is one of the most extensive mobile monitoring campaigns conducted in terms of the pollutants measured, the spatial coverage and resolution, and the campaign duration and sampling frequency.

2. METHODS

Repeated short-term measurements of TRAP, including particle number concentration (PNC), BC, NO_2, $PM_{2.5}$, and CO_2, were collected over a 1-year period at 309 roadside sites in the Puget Sound region. Sites were spatially and geographically similar to ACT cohort residences in the area. A temporally balanced, year-long driving schedule that measured TRAP during all seasons, days of the week, and most times of the day enabled us to estimate unbiased annual average estimates at the site level. Details are described below.

2.1. Spatial Compatibility of the Selected Roadside Sites and the ACT Cohort. We selected a mobile monitoring region in the greater Seattle, WA area that was roughly 1200 land km^2 (463 mi^2; Figure 1). The monitoring region was composed of Census Tracts where most of the ACT cohort (87% of the 11,904 locations) had historically resided between 1989 and 2018. This large region fell in western King County and southwest Snohomish County, and it included a variety of urban and rural areas with various land uses including residential, industrial, commercial, and downtown areas. We used the Location-Allocation tool in ArcMap (ArcGIS v. 10.5.1)[34] to select 304 sites within the monitoring region that were representative of the ACT cohort (approximately one monitoring site per 33 participant locations; see the Supporting Information [SI], Note S1 for details). Sites were spatially distributed so that they covered all parts of the monitoring region. The exact sites selected were meant to minimize the distance between the monitoring and cohort locations. Five additional sites were collocations at nearby agency air quality monitoring sites measuring pollutants similar to our platform (see details below). In total, there were 309 sites, most of which were on A4 (local and neighborhood roads; n = 282, 91%) and A3 (county and single-lane state highways; n = 27, 9%) roads. The average (SD) distance between a cohort location and the nearest monitoring site was 611 (397) m. The monitoring sites and cohort locations had similar distributions of various TRAP-related covariates (e.g., proximity to roadways, airport, railyard), indicating good spatial compatibility (Figure S1).[35]

2.2. Fixed Routes. We used ArcMap's Network Analyst New Route tool[34] and Google Maps[36] to develop nine fixed routes based on the 309 monitoring sites. Each route ranged from 75 to 168 km (47−104 mi) in length and had 28−40 sites (Table S1). All routes started and ended at the University of Washington and were intended to maximize residential driving coverage (i.e., reduce highway driving and driving on the same roads). Routes were downloaded from Google Maps to a smartphone and Garmin GPS Navigation System, and navigation was set to replicate the same route each time regardless of traffic conditions.

2.3. Sampling Schedule. Sampling was conducted from March 2019 through March 2020 during all seasons and days of the week between the hours of 5 AM and 11 PM. Our previous work has shown that this balanced but slightly reduced sampling schedule that takes driver safety and operational logistics into consideration should still generally produce unbiased annual averages.[27] This work further showed that the sampling temporality rather than the visit sampling duration has the largest impact on the accuracy of the annual average estimates and that common sampling designs like weekday business and rush hours regularly produce more biased annual averages. To increase temporal coverage, routes were started at different times of the day and driven in both clockwise and counterclockwise directions. A single route was driven each day (∼4−8 drive hours). Make-up site visits were conducted throughout the study to resample sites with missing readings (i.e., due to instrumentation or driver errors). Make-up visits occurred during similar times as the originally scheduled sampling time (i.e., season, day of the week, general time of day).

Twenty-eight 2 min samples were scheduled to be collected at each site while the vehicle was parked along the side of the road. This design choice was justified by our analyses of 1 min measurements from a near-road and a background agency site in Seattle. These analyses showed that at least 25 two-minute samples were sufficient to produce annual average estimates with a low average percent error (see Figure S2). There was only a negligible improvement in annual average estimates when the sampling duration was extended from 2 to 60 min.

2.4. Data Collection. We equipped a Toyota Prius hybrid vehicle with fast-response (1−60 s), high-quality instrumenta-

https://doi.org/10.1021/acs.est.2c01077
Environ. Sci. Technol. 2022, 56, 11460−11472

tion that measured various particles and gas pollutants. Pollutants included BC (AethLabs MA200), NO_2 (Aerodyne Research Inc. CAPS), $PM_{2.5}$ (Radiance Research M903 nephelometer), CO_2 (Li-Cor LI-850), and PNC with various instruments, including two TSI P-TRAK 8525s (one unscreened, the primary instrument in this analysis, and one with a diffusion screen), a TSI NanoScan 3910, and Testo DiSCmini. PNC serves as a surrogate for UFP since most particles by count are smaller than 100 nm.[37] The discussion further comments on the use of various PNC instruments. CO measurements were also collected, but these were not included in this analysis because they did not meet our quality standards. The platform additionally collected temperature, relative humidity, and global positioning with real-time tracking. Table S2 has instrumentation details, including the manufacturer-reported size ranges for the four PNC instruments. We had duplicates (back-ups) of every instrument type that were periodically collocated for quality assurance purposes (see Quality Assurance and Quality Control section). Note S2 and Figures S3 and S4 have additional details on the platform configuration and data collection procedures.

2.5. Quality Assurance and Quality Control. We conducted various quality assurance and quality control (QAQC) activities throughout the study period to ensure the reliability and integrity of our data. Activities included calibrating gas instruments; checking particle instruments for zero concentration responses; assessing collocated instruments for agreement; inspecting time series data for concentration pattern anomalies; and dropping readings associated with instrument error codes or those outside the instrument measurement range. Section S1.3 has additional details.

2.6. Site Visit Summaries. All data analyses were conducted in R (v 3.6.2, using RStudio v 1.2.5033; Note S3 has computing details).[38]

We calculated the median pollutant concentrations for each 2 min site visit. While means can be highly influenced by large concentration deviations (which may be important in some settings), medians are more robust to outliers and may better capture the typical values of skewed data.

We estimated $PM_{2.5}$ concentrations from nephelometer readings using a calibration curve fit to agency monitoring data between 1998 and 2017 (eq S1). Nephelometer light scattering is strongly correlated with $PM_{2.5}$ and has been used in the Puget Sound region to monitor air quality since 1967.[39] We fit the model using daily average measurements from nine nonindustrial agency air monitoring sites in the region where both $PM_{2.5}$ (using federal reference methods) and nephelometer light scattering data were collected. We excluded the years 2008−2009 due to nephelometer instrumentation issues noted by the local monitoring agency. The model's leave-one-site-out cross-validated R^2 and root mean square error (RMSE) were 0.92 and 1.97 $\mu g/m^3$, respectively.

Median visit and annual average concentrations for BC, NO_2, and $PM_{2.5}$ estimated from these data were compared against estimates from the five agency air monitoring collocation sites.

2.7. Spatial and Temporal Variability. We ran analysis of variance (ANOVA) models for each pollutant to characterize the breakdown of the total variability of the site visit-level data over space, time, and within the site. The dependent variable for each pollutant model was the median 2 min visit concentration (n = 8,697−8,999 measurements per pollutant), while the independent variables were the site (n = 309), day of the week (n = 7), hour of the day (n = 21), and season (n = 4) in that order. Any remaining variability (random or residual temporal) within a given site and time is captured by the residual term.

2.8. Estimation of Annual Averages. We calculated winsorized annual average concentrations for each site such that concentrations below the 5th and above the 95th quantile concentration were substituted with the 5th and 95th quantile concentrations, respectively (the mean of winsorized medians). This was done to reduce the influence of large outlier concentrations on the annual average. In sensitivity analyses, we calculated nonwinsorized averages (the mean of medians) and medians (the median of medians).

2.9. Annual Average Prediction Models. The development of annual average prediction models allows the predictions to be used for epidemiologic inference. The data were randomly split into a training-validation (90%, n = 278 sites) and a test (10%, n = 31 sites) set. The training-validation set was used to select the 191 geographic covariate predictors (e.g., land use, roadway proximity) that had sufficient variability and a limited number of outliers from 350 original covariates (see Note S5 for details). These were summarized using pollutant-specific partial least squares (PLS) regression components. We built pollutant-specific universal kriging (UK) models for annual average concentrations, using log-transformed concentrations as the dependent variable and the first three geocovariate PLS principal components as the independent variables (eq 1). We used UK rather than land use regression (LUR) alone since the UK uses geospatial smoothing to capture any residual spatial correlation not otherwise captured by LUR. Past work has used a similar UK-PLS modeling approach.[40,41] We selected the kriging variogram model for the geostatistical structure using the `fit.variogram` function in the `gstat`[42] R (v 3.6.2, using RStudio v 1.2.5033)[43] package. The models were

$$Log(Conc) = \alpha + \sum_{m=1}^{M} \theta_m Z_m + \varepsilon \quad (1)$$

where Conc is the pollutant concentration, Z_m is the PLS principal component scores (M = 3), α and θ_m are model coefficients, and ε is the residual term with mean zero and a modeled geostatistical structure.

We used RMSE and mean square error (MSE)-based R^2 to evaluate the performance of each pollutant model on the native scale using 10-fold cross-validation and the test sites. We used MSE-based R^2 instead of traditional, regression-based R^2 because it evaluates whether predictions and observations are the same (around the one-to-one line) such that it assesses both bias and variation around the one-to-one line. Regression-based R^2, on the other hand, solely assesses whether pairs of observations are linearly associated, regardless of whether observations are the same or not.

3. RESULTS

3.1. Data Collected. After dropping visit concentrations that did not meet the quality assurance standards (0.61%), the final analyses included over 70,000 2 min median visit measurements (almost 9000 samples per instrument) collected over the course of 288 drive days from 309 monitoring sites (Table S7). Sites were sampled an average of 29 times, ranging from 26 to 35 times. Due to the logistical constraints of sampling 309 sites with one platform along nine fixed routes,

https://doi.org/10.1021/acs.est.2c01077
Environ. Sci. Technol. 2022, 56, 11460−11472

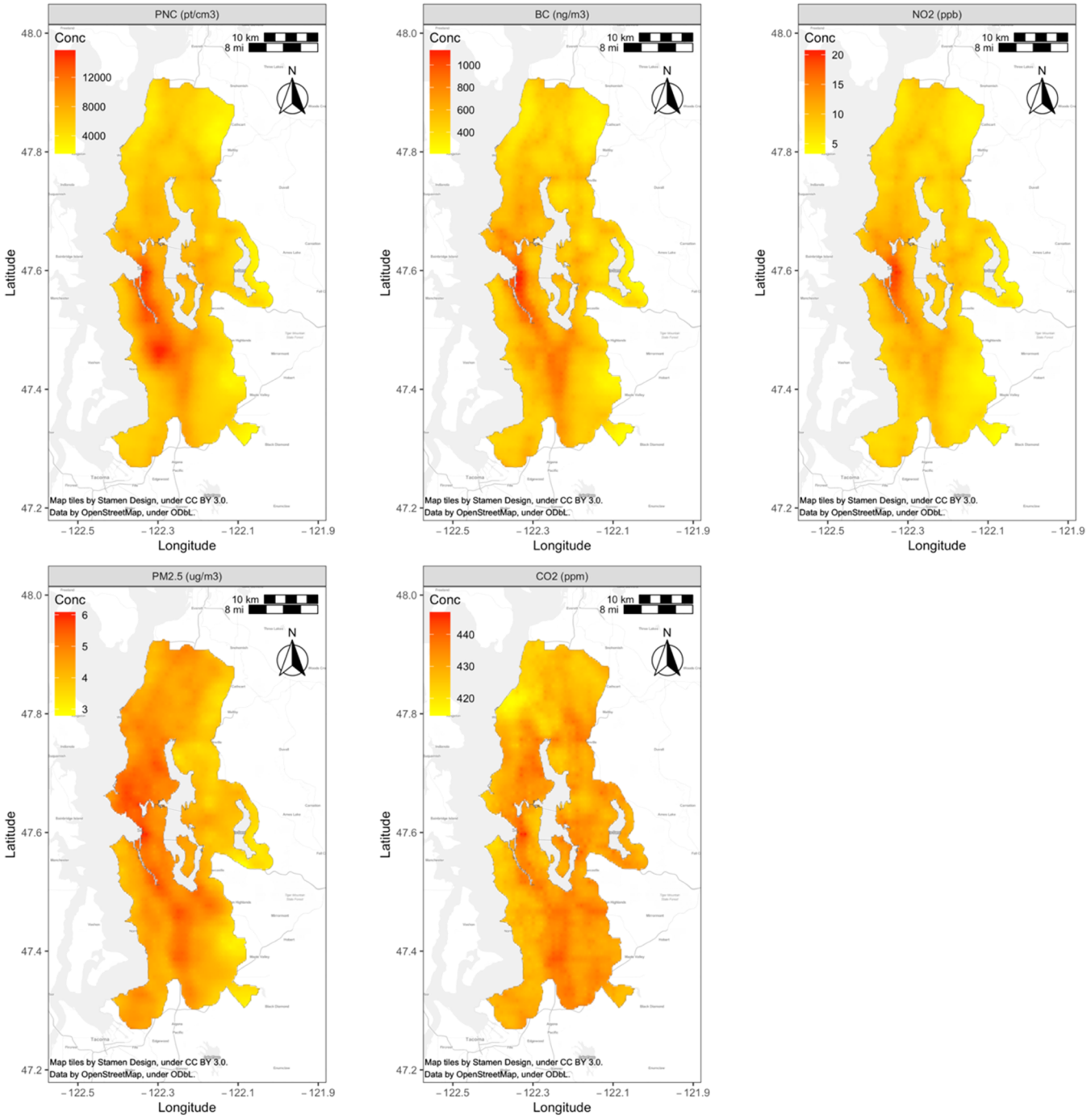

Figure 2. Pollutant prediction surfaces for the monitoring region.

some sites were visited fewer times of the day than other sites, though sampling times were still well distributed throughout the day (e.g., morning, afternoon, and evening; see Figure S7). Site Visits in the SI, Section S2.1 have additional details on the visit-level pollutant concentrations used to estimate site annual averages.

3.2. Quality Assurance and Quality Control. Median 2 min BC, NO_2, and $PM_{2.5}$ measurements from mobile monitoring were generally in agreement with measurements from agency sites (MSE-based R^2: BC = 0.69, NO_2 = 0.71, $PM_{2.5}$ = 0.61; Figure S12). Annual average estimates from our mobile monitoring campaign measurements were similar to annual average estimates from comparable 2 min samples at collocation agency monitoring sites, and these were in moderate agreement with the true annual average concentrations at those sites based on all of the available data during the study period (Figure S13).

While we were unable to compare CO_2 or PNC measurements to regulatory or agency-operated observations, duplicate instrument collocations generally showed good agreement (Figure S6). Additionally, CO_2 instruments performed well during periodic calibration assessments and PNC instruments during zero checks (Table S3, Figure S5).

3.3. Spatial and Temporal Variability. We conducted pollutant-specific ANOVA analyses of winsorized site visit concentrations to characterize the relative spatial and temporal

https://doi.org/10.1021/acs.est.2c01077
Environ. Sci. Technol. 2022, 56, 11460−11472

variability of the 2 min concentrations. These results indicated that most of the concentration variability occurred within sites rather than across sites or over time (Figure S14). PNC had the most spatial variability (17%), followed by NO_2 (12%), BC (8%), CO_2 (5%), and $PM_{2.5}$ (2%). Unlike other pollutants, PNC had more spatial than temporal variability. CO_2 (27%) had the most temporal variability, followed by NO_2 (24%), BC (17%), $PM_{2.5}$ (14%), and PNC (7%). After accounting for the site and time, $PM_{2.5}$ had the highest within-site variability (i.e., random or residual temporal variability; 84% of the total), followed by PNC from the P-TRAK (76%), BC (75%), CO_2 (69%), and finally, NO_2 (64%). Figure S14 shows similar results for other PNC instruments.

3.4. Annual Average Estimates. Estimated annual average pollutant concentrations across all monitoring sites are shown in Figure S15. There was a four to sixfold difference between the lowest and highest site concentrations of PNC, NO_2, and BC. On the other hand, $PM_{2.5}$ had a twofold difference across sites, while CO_2 varied little across sites. Among PNC instruments, the screened P-TRAK measured the lowest concentrations and had the smallest variability; the P-TRAK, which did not screen out particles below 36 nm, had the second-highest averages with approximately double the values and more variability. The DisSCmini and Nanoscan had higher medians, more variability, and more outlying annual average concentrations. Figures S16 and S17 map these concentrations. The locations with the highest BC, NO_2, and PNC concentrations were near the Seattle urban core. High PNC concentration sites were additionally located at more southern locations near the area's major airport, the Seattle-Tacoma (Sea-Tac) International Airport. Sites with elevated $PM_{2.5}$ and CO_2 levels were dispersed throughout the monitoring region.

3.5. Prediction Models. Based on the training-validation set, the first three PLS principal components captured between 49 and 51% of the observed concentration variability for each pollutant model. Loadings from the first PLS principal component indicated that the normalized difference vegetation index (NDVI), length of bus routes, major roadways, land development, population density, and truck routes were strong predictors of air pollution in the region, with some pollutants, for example, PNC, being more influenced by these land features (Figure S18). Cross-validated MSE-based R^2 (and RMSE) values for UK-PLS models were 0.77 (1,177 pt/cm^3) for PNC, 0.60 (102 ng/m^3) for BC, 0.77 (1.3 ppb) for NO_2, 0.70 (0.3 μg/m^3) for $PM_{2.5}$, and 0.51 (4.2 ppm) for CO_2 (Table S9). In the independent test set, these results differed somewhat with estimates of MSE-based R^2 (and RMSE) of 0.78 (815 pt/cm^3) for PNC, 0.80 (60 ng/m^3) for BC, 0.84 (0.9 ppb) for NO_2, 0.73 (0.3 μg/m^3) for $PM_{2.5}$, and 0.77 (2.7 ppm) for CO_2. Sensitivity analyses using the mean of median and the median of median annual averages performed similarly or slightly lower due to changes in the number of influential points and/or reduced overall variability (Table S9). These model performances are reflected in the generally good agreement between the estimates and cross-validated predictions. Figure S19 compares site estimates to their respective model predictions and shows that most of the predictions are evenly scattered around the 1−1 line (not systematically biased) and that predictions are generally within 25% of the observed values. There were a few high PNC observations that were underpredicted by the models by more than 25%.

Model predictions for the monitoring region are shown in Figure 2. While $PM_{2.5}$ and CO_2 are fairly spatially homogeneous, PNC, BC, and NO_2 (traditional TRAPs) show higher concentrations in the urban core and along major roads. In addition, PNC shows a higher concentration near the area's major airport. All of the PNC instruments reflect this broad pattern, although there are differences across instruments in the areas with the highest predicted concentrations (Figure S20).

Pearson correlation coefficients (R) between all pollutant model predictions at the 309 monitoring sites are shown in Figure S21. Different PNC instruments were generally well correlated with each other (R = 0.85−0.97). Overall, PNC from the P-TRAK, BC, and NO_2 was well correlated with each other (R = 0.81−0.92) and moderately correlated with $PM_{2.5}$ and CO_2 (R = 0.39−0.70). CO_2 and $PM_{2.5}$ were moderately correlated with each other (R = 0.46). The biggest deviations from a linear association were evident for the predicted high concentrations from the DiSCmini; this was particularly apparent in its relationship with BC (R = 0.72), NO_2 (R = 0.68), $PM_{2.5}$ (R = 0.38), and CO_2 (R = 0.29).

4. DISCUSSION

In this paper, we describe the design of an innovative mobile monitoring campaign specifically developed to estimate relatively unbiased, highly spatially resolved, long-term TRAP exposures in an epidemiologic cohort. To date, this is one of the most extensive mobile monitoring campaigns conducted in terms of the pollutants measured (five pollutants measured with eight different instruments, not including CO) spatial coverage (~1200 land km^2), sampling density (309 monitoring sites along nine routes or 1 monitor every 3.9 land km^2), and sampling frequency (7 days a week; 288 days over a 1-year period) and duration (~5 driving hours per day between the hours of 5 AM and 11 PM). The spatial resolution achieved by this campaign was significantly greater than would be expected from fixed agency monitoring approaches. We had one monitor per 3.9 km^2 of the land area rather than 183 km^2 (there were six agency sites in the monitoring area), almost a 50-fold increase. Furthermore, these monitoring locations were carefully selected to be as representative as possible of our population of interest, the ACT cohort, and this included the decision to collect stationary samples off the side of the road rather than purely rely on roadway data collected while in driving. The average (SD) distance from an ACT cohort location to the nearest monitoring site was 611 (397) m rather than 5805 (2805) m to an AQS site, almost a 10-fold difference. Monitor proximity to prediction (i.e., cohort) locations, both in terms of geographic and covariate distance, is an important determinant of accurate exposure assessment.[44,45] For instance, closer monitor proximity to prediction sites can improve UK model predictions since these incorporate spatial correlation into LUR predictions. Additionally, we previously showed that more temporally balanced sampling across hours, days of the week, and seasons is expected to produce more accurate and largely unbiased annual average estimates as compared to more common campaigns with reduced temporal coverage.[27]

A unique aspect of this campaign was the collection of stationary samples along the side of the road. While most other campaigns have only collected nonstationary, on-road samples, various studies have shown that mobile samples are generally higher in concentration than stationary samples.[21,46−49] It has

https://doi.org/10.1021/acs.est.2c01077
Environ. Sci. Technol. 2022, 56, 11460−11472

not yet been documented how to responsibly use nonstationary data in epidemiologic applications. Among the relatively few campaigns that have collected stationary rather than mobile measurements alone, most have sampled for longer than 2 min (about 15−60 min per measurement).[50] Our analyses indicated that shorter sampling periods produce comparably good estimates without adding excessive amounts of stationary sampling time to mobile monitoring campaigns (Figure S2). Our use of a hybrid vehicle meant that the vehicle was operating by a battery with the engine off during roadside stop measurement periods, thus reducing the possibility of self-contamination.

ANOVA model results indicate differences across pollutants in terms of their spatial and temporal variability. This finding is particularly relevant for short-term mobile monitoring campaigns, which can be designed to adequately capture the variability of the pollutants of interest. These findings suggest that repeated sampling at any given site is crucial since most of the variability for all measured pollutants was seen within sites, even after adjusting for predictable temporal factors (season, day of week, and hour of day). Following that, all pollutants other than PNC had relatively more temporal than spatial variability. Campaigns measuring these pollutants may thus benefit by inclusion of more temporally balanced site visits. PNC, on the other hand, has slightly more spatial than temporal variability, suggesting that both are important. The implementation of these concepts for epidemiologic exposure assessment should translate to reduced exposure misclassification. Overall, our results are in line with past literature that has shown differing spatial and temporal contrasts across pollutants,[51,52] though our work increases the robustness of these findings using a more spatially resolved, multipollutant dataset that includes less commonly measured PNC.

The findings from this campaign demonstrate the region's generally low air pollution levels that result from relatively low regional emissions of TRAP. The ranges of annual concentrations across sites for $PM_{2.5}$ (3.3−6.3 $\mu g/m^3$) and NO_2 (3.9−23 ppb) were well below the National Ambient Air Quality Standards (NAAQS) annual average levels of 12 $\mu g/m^3$ and 53 ppb, respectively.[53] Mean annual PNC (~7000 [range: 4000−18,000] pt/cm^3) and BC (~600 [range: 270−1,500] ng/m^3) site concentrations were lower than what others have reported in cities throughout the world where mean study values range from roughly 6000−47,000 PNC pt/cm^3 and 400−14,000 BC ng/m^3 (PNC;[21,47,48,54−67] BC[19,21,48,57,58,63,67−79]). While CO_2 site concentrations (416−455 ppm) were above the 2019 global average of 412 ppb,[80] they were in line with past work noting elevated carbon footprint levels in dense, high-income cities and affluent suburbs.[81,82] Still, the high concentration variability seen across sites for pollutants like PNC, BC, and NO_2 suggests that future epidemiological cohort analyses may have more power to observe health effects from these pollutants than those that are less spatially variable, for example, $PM_{2.5}$ and CO_2.

The similarity between BC, NO_2, and $PM_{2.5}$ measurements from our campaign and collocated agency monitoring sites confirms that our campaign estimates were generally accurate. Some of the discrepancies between the two monitoring approaches may be due to differences in the sampling instrumentation, the exact sampling location, and quality assurance and quality control procedures. Furthermore, duplicate CO_2 and PNC instrument collocations generally showed good agreement (Figure S6). CO_2 calibrations and PNC zero checks additionally showed good performance (Table S3, Figure S5).

We observed elevated annual average pollutant levels near areas with low green space (as quantified by NDVI), bus routes, major roadways, and impervious surfaces. These findings are generally in line with past work.[83]

While future mobile monitoring campaigns may be guided by the design and findings from this study, it is notable that the unique geographical, meteorological, and source characteristics of different airsheds may produce slightly different results. These results do highlight, however, the importance of collecting multipollutant measurements, particularly in urban or other areas characterized by major emission sources such as airports or railroad systems, which may be important contributors to local and/or regional air pollution levels. This is particularly true for PNC given the limited monitoring data available and its unique spatial and temporal patterns. More generally, multipollutant exposure assessment is a growing interest in the field of air pollution epidemiology.[51,84−87]

While UFPs are generally characterized as particles under 100 nm in diameter, this definition is not standardized and varies from instrument to instrument as well as study to study. Since most particles by count are in the smaller size range with few above 100 nm,[37] PNC should adequately characterize UFPs. Moreover, the collection of PNC from multiple instruments in a field setting is unique to this study. PNC measures from different instruments were strongly correlated with each other, and they produced broadly similar spatial surfaces, strengthening our confidence in the quality of our measurements. Differences in the reported PNC levels across instruments, however, can be attributed to multiple factors including differences in technology, each technology's unique particle size detection efficacy, and built-in calibration (if present), all of which impact the reported particle size ranges and concentrations of each instrument. Differences across PNC instruments in the predicted absolute concentrations as well as overall spatial surfaces highlight these differences. By comparing PNC levels from the unscreened and screened P-TRAK, for example, we see that roughly half of the measured (and predicted) particles are between 20 and 36 nm (Figure S20). Furthermore, these smaller particles are more concentrated near the area's major airport, the Sea-Tac International Airport. The DiSCmini also captures this rise in PNC near the airport but shows much lower relative concentrations elsewhere, suggesting that it measures smaller particles well. Reasons could include the different measurement technology as well as the manufacturer's reported lower particle size cut of 10 nm. The NanoScan total concentration, on the other hand, reports concentrations that are roughly 50% higher than the unscreened P-TRAK, with elevated PNC levels near the airport, but also in other parts of the monitoring region, including south of the airport along major roadways and at the Seattle urban core. Elevated PNC levels are thus predicted from the NanoScan in a larger area of the monitoring region. It is not initially clear from this analysis why the P-TRAK may result in less spatially variable results across time periods when compared to other instruments (Figures S8−S11). Knowing that this instrument (although popular in the field) does not effectively capture very small particles (<20 nm), we hypothesize that these smallest particles are much more variable in space. This might explain why we see more variability in the NanoScan and DiSCmini, both of which have

https://doi.org/10.1021/acs.est.2c01077
Environ. Sci. Technol. 2022, 56, 11460−11472

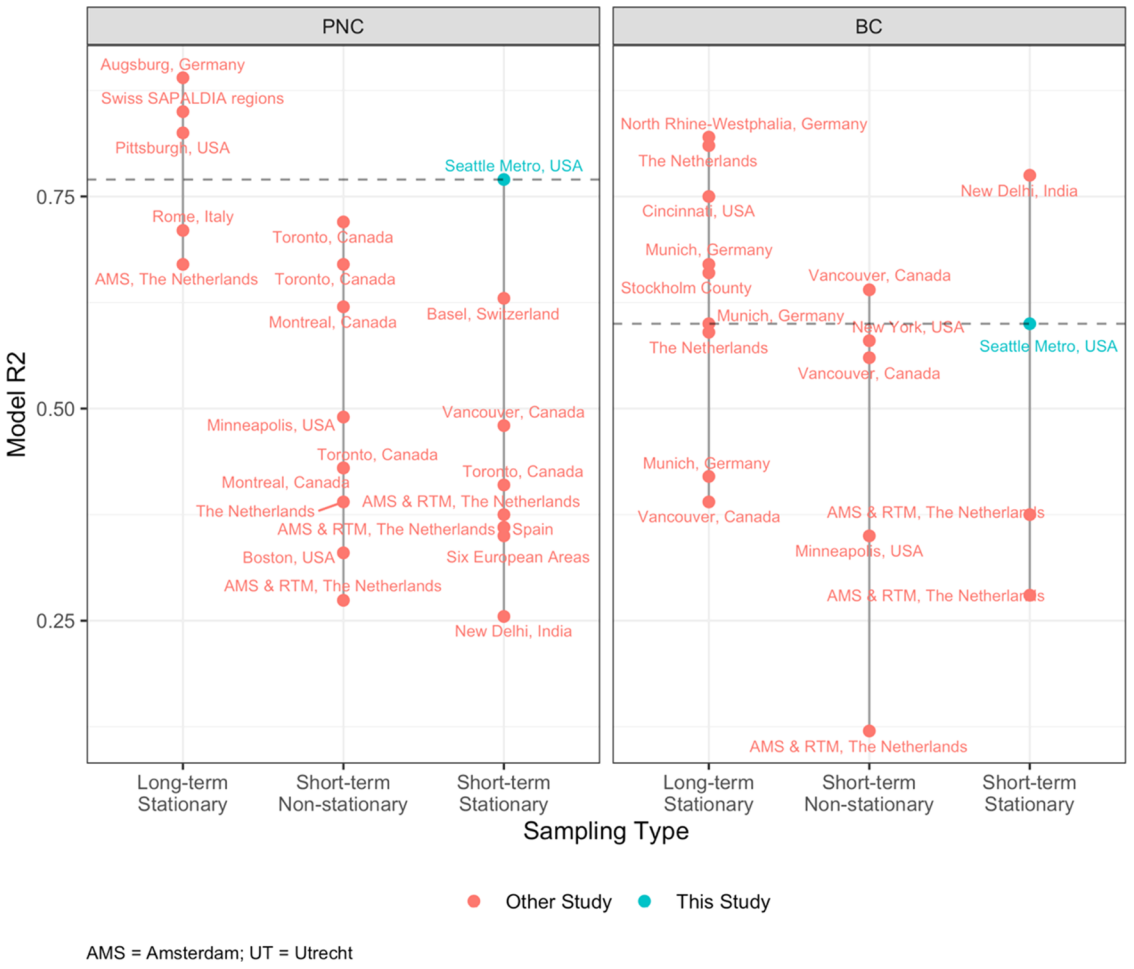

Figure 3. Cross-validated model R^2 estimates from this study and other PNC[21,47,48,54,55,58−67,72,89−94,96] and BC[21,58,63,67−79] studies. Studies are stratified by whether the sampling type was traditional, fixed-site sampling (long-term stationary), short-term mobile monitoring campaigns that collected on-road data while in motion (short-term nonstationary), or short-term mobile monitoring campaigns that collected data while stopped (short-term stationary). The figure does not include Saha et al. (2021),[95] who used a mixed sampling approach for PNC from multiple sources (R^2: 0.54−0.72). The horizontal dashed line is the R^2 for this study. Plots show the average R^2 from a study if multiple models were presented without a clear primary model.

lower size cuts of 10 nm. The greater spatial variability of these smallest particles is consistent with the spatial variability of the likely sources of the smallest UFPs and their rapid agglomeration to larger sizes. Without conducting a more in-depth particle size distribution analysis (for example, in a controlled chamber environment), however, it is unclear exactly which instrument features impact the reported measurements and to what degree.

It is an open question whether the use of different PNC instruments across epidemiologic studies makes cross-study comparisons and coherent causal determinations difficult or whether these differences still produce interpretable findings for the field as a whole.[88] We observed, for example, a slightly nonlinear relationship between the DiSCmini and all other PNC instruments when the predicted concentrations were high (Figure S21). A nonlinear trend was also present when comparing the BC, NO_2, $PM_{2.5}$, and CO_2 predictions to those from the DiSCmini but less so when comparing these to the PNC predictions from other instruments. Furthermore, we will be able to characterize size-specific exposure surfaces, sources, and health effects by using size-resolved particle counts from the NanoScan (13 size bins, data not shown) or by looking at the differences between the unscreened and screened P-TRAKs, where the minimum sizes are 20 and 36 nm, respectively.

A feature of mobile monitoring campaigns is their reliance on repeated, short-term samples to achieve increased spatial coverage when compared to traditional long-term monitoring approaches. Since we collected about 29 2 min samples from each of our 309 sites (about an hour of data at each site), we recognize that the resulting annual average site estimates are noisy. Still, with MSE-based R^2 values of 0.77 for PNC and 0.60 for BC, our models performed better than many other models that are based on short-term stationary and nonstationary monitoring campaigns (R^2 of approximately 0.13−0.72 for PNC[21,47,48,54,55,58−61,63−67,72,89−95] and 0.12−0.86 for BC).[21,58,63,67,72,75,76,79] While other design features across studies could be responsible for some of the variability in R^2 values, Figure 3 shows that (traditional) long-term stationary monitoring studies almost always perform better than both short-term nonstationary and stationary monitoring, both of which perform like one another. Our performance is clearly higher than the bulk of other short-term stationary studies for PNC and near the higher end of the performance scale for BC. This improved performance is important given the cost and

https://doi.org/10.1021/acs.est.2c01077
Environ. Sci. Technol. 2022, 56, 11460−11472

challenges of measuring PNC using stationary sampling designs.

Figures S22 and S23 highlight some important monitoring design features that are unique to this study, which we hypothesize are responsible for our improved performances. For PNC, Saha et al. (2019) reported that studies that collect short-term stationary samples like ours have generally sampled between 60 and 644 sites, sampled each site between 15 min and 3 h at a time, and visited each site between 1 and 5 times. Similarly, BC studies like this one have generally sampled 26−161 sites, sampled each site for about 30 min, and visited each site about 2−3 times. Campaigns with more sites have generally collected fewer repeat site visits. Since we visited each site for shorter periods of time (2 min), this allowed us to collect more repeat site visits (approximately 29) at more sites (309) than what most short-term stationary studies have achieved. While our resulting total site sampling durations (∼58 min) were similar to other short-term stationary studies, we captured more temporal variability by sampling year-around during all days of the week and most times of the day, a limitation of most past campaigns. In terms of our modeling approach, we focused on annual average site concentrations from winsorized observations. This is a longer averaging period than what most other studies have reported and one that reduces the variability of the observations to focus on the spatial contrasts of interest. This could have resulted in better performing models than had we modeled concentrations without aggregating them to annual averages. Additionally, some of the models compared here are spatiotemporal approaches that model shorter-term repeated measures rather than longer-term site averages. This is in line with past work showing that mobile models can sometimes poorly explain their own noisy measurements, but that the same model can better explain more stable longer-term concentrations.[21,27,97]

This impact of concentration variability on model performances is seen in our sensitivity analyses. Calculating annual averages from nonwinsorized observations, for example, generally resulted in slightly lower-performing PNC and $PM_{2.5}$ models due to the inclusion of more influential points in the models. Using a measure more robust to extreme observations, the annual average median produced lower-performing CO_2 models due to the further reduction in variability. Still, we reported good out-of-sample MSE-based R^2 estimates, which better characterize a model's predictive performance at new locations and are generally lower than the in-sample regression-based R^2 estimates that many studies report. We estimated these higher model performances despite the lower air pollution levels in our monitoring region, which can make it harder to get good prediction performance due to reduced variability (e.g., CO_2 and $PM_{2.5}$).

Finally, our monitoring network was larger and denser than most similar studies. This allowed us to better capture the concentration variability across a larger geographic area, which included hotspots that may have otherwise been missed by more sparse monitoring networks.

When thinking about epidemiologic application, this 2019−2020 surface may be sufficient for assessing cohort exposures near this time. Air pollution studies generally use shorter-term exposure as an indicator of longer-term exposure,[5] although a few have developed methods for extrapolating surfaces over time.[7−14] Exposure assessment using the models developed in this study will need to be justified by the specific epidemiologic investigation.

Overall, these results demonstrate how this campaign design captured the spatial pollutant variations in the region. We expect that these data will produce robust and representative annual average TRAP exposures for the ACT cohort and that this type of design should be considered for future epidemiologic cohort applications. The next steps include applying these prediction models to the cohort and conducting inferential analyses to determine the association of these pollutants with brain health. The rich dataset from this extensive campaign also provides an excellent foundation for investigating many important questions about how to best design mobile monitoring campaigns for application to subsequent epidemiologic studies.

■ ASSOCIATED CONTENT

Supporting Information

The Supporting Information is available free of charge at https://pubs.acs.org/doi/10.1021/acs.est.2c01077.

Mobile monitoring campaign description, protocols, and QAQC; summary estimate and prediction results presented in tables and figures (PDF)

■ AUTHOR INFORMATION

Corresponding Author

Magali N. Blanco − *Department of Environmental and Occupational Health Sciences, School of Public Health, University of Washington, Hans Rosling Center for Population Health, Seattle, Washington 98195, United States;* orcid.org/0000-0002-9998-995X; Email: magali@uw.edu

Authors

Amanda Gassett − *Department of Environmental and Occupational Health Sciences, School of Public Health, University of Washington, Hans Rosling Center for Population Health, Seattle, Washington 98195, United States*

Timothy Gould − *Department of Civil & Environmental Engineering, College of Engineering, University of Washington, Seattle, Washington 98195, United States*

Annie Doubleday − *Department of Environmental and Occupational Health Sciences, School of Public Health, University of Washington, Hans Rosling Center for Population Health, Seattle, Washington 98195, United States*

David L. Slager − *Department of Environmental and Occupational Health Sciences, School of Public Health, University of Washington, Hans Rosling Center for Population Health, Seattle, Washington 98195, United States*

Elena Austin − *Department of Environmental and Occupational Health Sciences, School of Public Health, University of Washington, Hans Rosling Center for Population Health, Seattle, Washington 98195, United States;* orcid.org/0000-0002-4724-1042

Edmund Seto − *Department of Environmental and Occupational Health Sciences, School of Public Health, University of Washington, Hans Rosling Center for Population Health, Seattle, Washington 98195, United States*

Timothy V. Larson − *Department of Environmental and Occupational Health Sciences, School of Public Health, University of Washington, Hans Rosling Center for Population Health, Seattle, Washington 98195, United States; Department of Civil & Environmental Engineering,*

College of Engineering, University of Washington, Seattle, Washington 98195, United States

Julian D. Marshall − *Department of Civil & Environmental Engineering, College of Engineering, University of Washington, Seattle, Washington 98195, United States;* orcid.org/0000-0003-4087-1209

Lianne Sheppard − *Department of Environmental and Occupational Health Sciences, School of Public Health, University of Washington, Hans Rosling Center for Population Health, Seattle, Washington 98195, United States; Department of Biostatistics, School of Public Health, University of Washington, Hans Rosling Center for Population Health, Seattle, Washington 98195, United States*

Complete contact information is available at: https://pubs.acs.org/10.1021/acs.est.2c01077

Notes

The authors declare no competing financial interest.

■ ACKNOWLEDGMENTS

The authors are grateful to their two drivers, Jim Sullivan and Dave Hardie, for all of their efforts collecting these data and to Brian High for building and supporting the database. This work was funded by the Adult Changes in Thought-Air Pollution (ACT-AP) Study (National Institute of Environmental Health Sciences [NIEHS], National Institute on Aging [NIA], R01ES026187), BEBTEH: Biostatistics, Epidemiologic, & Bioinformatic Training in Environmental Health (NIEHS, T32ES015459), and the University of Washington Interdisciplinary Center for Exposure, Disease, Genomics, & Environment (NIEHS, 2P30 ES007033-26). The research described in this article was conducted in part under contract to the Health Effects Institute (HEI), an organization jointly funded by the United States Environmental Protection Agency (EPA) (Assistance Award No. CR-83998101), and certain motor vehicle and engine manufacturers. The contents of this article do not necessarily reflect the views of HEI, or its sponsors, nor do they necessarily reflect the views and policies of the EPA or motor vehicle and engine manufacturers.

■ REFERENCES

(1) Brunekreef, B.; Holgate, S. T. Air Pollution and Health. *Lancet* **2002**, *360*, 1233−1242.

(2) Allen, J. L.; Klocke, C.; Morris-Schaffer, K.; Conrad, K.; Sobolewski, M.; Cory-Slechta, D. A. Cognitive Effects of Air Pollution Exposures and Potential Mechanistic Underpinnings. *Curr. Environ. Health Rep.* **2017**, 180−191.

(3) Kilian, J.; Kitazawa, M. The Emerging Risk of Exposure to Air Pollution on Cognitive Decline and Alzheimer's Disease - Evidence from Epidemiological and Animal Studies. *Biomed. J.* **2018**, *41*, 141−162.

(4) Power, M. C.; Adar, S. D.; Yanosky, J. D.; Weuve, J. Exposure to Air Pollution as a Potential Contributor to Cognitive Function, Cognitive Decline, Brain Imaging, and Dementia: A Systematic Review of Epidemiologic Research. *Neurotoxicology* **2016**, *56*, 235−253.

(5) Weuve, J.; Bennett, E. E.; Ranker, L.; Gianattasio, K. Z.; Pedde, M.; Adar, S. D.; Yanosky, J. D.; Power, M. C. Exposure to Air Pollution in Relation to Risk of Dementia and Related Outcomes: An Updated Systematic Review of the Epidemiological Literature. *Environ. Health Perspect.* **2021**, *129*, No. 096001.

(6) Delgado-Saborit, J. M.; Guercio, V.; Gowers, A. M.; Shaddick, G.; Fox, N. C.; Love, S. A Critical Review of the Epidemiological Evidence of Effects of Air Pollution on Dementia, Cognitive Function and Cognitive Decline in Adult Population. *Sci. Total Environ.* **2021**, *757*, No. 143734.

(7) Karner, A. A.; Eisinger, D. S.; Niemeier, D. A. Near-Roadway Air Quality: Synthesizing the Findings from Real-World Data. *Environ. Sci. Technol.* **2010**, *44*, 5334−5344.

(8) Seaton, A.; Godden, D.; MacNee, W.; Donaldson, K. Particulate Air Pollution and Acute Health Effects. *Lancet* **1995**, *345*, 176−178.

(9) Lundborg, M.; Johard, U.; Låstbom, L.; Gerde, P.; Camner, P. Human Alveolar Macrophage Phagocytic Function Is Impaired by Aggregates of Ultrafine Carbon Particles. *Environ. Res.* **2001**, *86*, 244−253.

(10) Stone, V.; Tuinman, M.; Vamvakopoulos, J. E.; Shaw, J.; Brown, D.; Petterson, S.; Faux, S. P.; Borm, P.; MacNee, W.; Michaelangeli, F.; Donaldson, K. Increased Calcium Influx in a Monocytic Cell Line on Exposure to Ultrafine Carbon Black. *Eur. Respir. J.* **2000**, *15*, 297−303.

(11) Li, N.; Sioutas, C.; Cho, A.; Schmitz, D.; Misra, C.; Sempf, J.; Wang, M.; Oberley, T.; Froines, J.; Nel, A. Ultrafine Particulate Pollutants Induce Oxidative Stress and Mitochondrial Damage. *Environ. Health Perspect.* **2003**, *111*, 455−460.

(12) Donaldson, K. Ultrafine Particles. *Occup. Environ. Med.* **2001**, *58*, 211−216.

(13) Brown, D. M.; Wilson, M. R.; MacNee, W.; Stone, V.; Donaldson, K. Size-Dependent Proinflammatory Effects of Ultrafine Polystyrene Particles: A Role for Surface Area and Oxidative Stress in the Enhanced Activity of Ultrafines. *Toxicol. Appl. Pharmacol.* **2001**, *175*, 191−199.

(14) Oberdorster, G.; Ferin, J.; Lehnert, B. E. Correlation between Particle Size, in Vivo Particle Persistence, and Lung Injury. *Environ. Health Perspect.* **1994**, *102 Suppl 5*, 173−179.

(15) US EPA. *Overview of the Clean Air Act and Air Pollution*. United States Environmental Protection Agency (US EPA). https://www.epa.gov/clean-air-act-overview (accessed April 23, 2021).

(16) Li, H. Z.; Gu, P.; Ye, Q.; Zimmerman, N.; Robinson, E. S.; Subramanian, R.; Apte, J. S.; Robinson, A. L.; Presto, A. A. Spatially Dense Air Pollutant Sampling: Implications of Spatial Variability on the Representativeness of Stationary Air Pollutant Monitors. *Atmos. Environ. X* **2019**, *2*, No. 100012.

(17) US Census. *TIGER/Line Shapefile, 2017, 2010 Nation, U.S., 2010 Census Urban Area National*, 2021.

(18) US EPA. *AirData Pre-Generated Data Files*. US Environmental Protection Agency. https://aqs.epa.gov/aqsweb/airdata/download_files.html (accessed Dec 07, 2019).

(19) Apte, J. S.; Messier, K. P.; Gani, S.; Brauer, M.; Kirchstetter, T. W.; Lunden, M. M.; Marshall, J. D.; Portier, C. J.; Vermeulen, R. C. H.; Hamburg, S. P. High-Resolution Air Pollution Mapping with Google Street View Cars: Exploiting Big Data. *Environ. Sci. Technol.* **2017**, *51*, 6999−7008.

(20) Hatzopoulou, M.; Valois, M. F.; Levy, I.; Mihele, C.; Lu, G.; Bagg, S.; Minet, L.; Brook, J. Robustness of Land-Use Regression Models Developed from Mobile Air Pollutant Measurements. *Environ. Sci. Technol.* **2017**, *51*, 3938−3947.

(21) Kerckhoffs, J.; Hoek, G.; Messier, K. P.; Brunekreef, B.; Meliefste, K.; Klompmaker, J. O.; Vermeulen, R. Comparison of Ultrafine Particle and Black Carbon Concentration Predictions from a Mobile and Short-Term Stationary Land-Use Regression Model. *Environ. Sci. Technol.* **2016**, *50*, 12894−12902.

(22) Patton, A. P.; Perkins, J.; Zamore, W.; Levy, J. I.; Brugge, D.; Durant, J. L. Spatial and Temporal Differences in Traffic-Related Air Pollution in Three Urban Neighborhoods near an Interstate Highway. *Atmos. Environ.* **2014**, *99*, 309−321.

(23) Van den Bossche, J.; Peters, J.; Verwaeren, J.; Botteldooren, D.; Theunis, J.; De Baets, B. Mobile Monitoring for Mapping Spatial Variation in Urban Air Quality: Development and Validation of a Methodology Based on an Extensive Dataset. *Atmos. Environ.* **2015**, *105*, 148−161.

(24) Whitby, K. T.; Clark, W. E.; Marple, V. A.; Sverdrup, G. M.; Sem, G. J.; Willeke, K.; Liu, B. Y. H.; Pui, D. Y. H. Characterization of

California Aerosols-I. Size Distributions of Freeway Aerosol. *Atmos. Environ.* **1975**, *9*, 463−482.
(25) Xie, X.; Semanjski, I.; Gautama, S.; Tsiligianni, E.; Deligiannis, N.; Rajan, T. R.; Pasveer, F.; Philips, W. A Review of Urban Air Pollution Monitoring and Exposure Assessment Methods. *ISPRS Int. J. Geo-Inf.* **2017**, *6*, No. 389.
(26) Alexeeff, S. E.; Roy, A.; Shan, J.; Liu, X.; Messier, K.; Apte, J. S.; Portier, C.; Sidney, S.; Eeden, S. K. V. D. High-Resolution Mapping of Traffic Related Air Pollution with Google Street View Cars and Incidence of Cardiovascular Events within Neighborhoods in Oakland, CA. *Environ. Health* **2018**, *17*, No. 38.
(27) Blanco, M. N.; Doubleday, A.; Austin, E.; Marshall, J. D.; Seto, E.; Larson, T.; Sheppard, L. Design and Evaluation of Short-Term Monitoring Campaigns for Long-Term Air Pollution Exposure Assessment. *J. Expo. Sci. Environ. Epidemiol.* DOI: 10.1101/2021.04.21.21255641.
(28) Klompmaker, J. O.; Montagne, D. R.; Meliefste, K.; Hoek, G.; Brunekreef, B. Spatial Variation of Ultrafine Particles and Black Carbon in Two Cities: Results from a Short-Term Measurement Campaign. *Sci. Total Environ.* **2015**, *508*, 266−275.
(29) Montagne, D. R.; Hoek, G.; Klompmaker, J. O.; Wang, M.; Meliefste, K.; Brunekreef, B. Land Use Regression Models for Ultrafine Particles and Black Carbon Based on Short-Term Monitoring Predict Past Spatial Variation. *Environ. Sci. Technol.* **2015**, *49*, 8712−8720.
(30) Riley, E. A.; Banks, L.; Fintzi, J.; Gould, T. R.; Hartin, K.; Schaal, L. N.; Davey, M.; Sheppard, L.; Larson, T.; Yost, M. G.; Simpson, C. D. Multi-Pollutant Mobile Platform Measurements of Air Pollutants Adjacent to a Major Roadway. *Atmos. Environ.* **2014**, *98*, 492−499.
(31) Wai, T. H.; Apte, J. S.; Harris, M. H.; Kirchstetter, T. W.; Portier, C. J.; Preble, C. V.; Roy, A.; Szpiro, A. A. Insights from Application of a Hierarchical Spatio-Temporal Model to an Intensive Urban Black Carbon Monitoring Dataset. *Atmos. Environ.* **2022**, *277*, No. 119069.
(32) Alexeeff, S. E.; Roy, A.; Shan, J.; Liu, X.; Messier, K.; Apte, J. S.; Portier, C.; Sidney, S.; Eeden, S. K. Van. Den. High-Resolution Mapping of Traffic Related Air Pollution with Google Street View Cars and Incidence of Cardiovascular Events within Neighborhoods in Oakland, CA. *Environ. Health* **2018**, *17*, No. 38.
(33) Kukull, W. A.; Higdon, R.; Bowen, J. D.; McCormick, W. C.; Teri, L.; Schellenberg, G. D.; Van Belle, G.; Jolley, L.; Larson, E. B. Dementia and Alzheimer Disease Incidence: A Prospective Cohort Study. *Arch. Neurol.* **2002**, *59*, 1737−1746.
(34) Esri. *ArcGIS Desktop*. https://www.esri.com/ (accessed April 26, 2021).
(35) Szpiro, A. A.; Paciorek, C. J. Measurement Error in Two-Stage Analyses, with Application to Air Pollution Epidemiology. *Environmetrics* **2013**, *24*, 501−517.
(36) Google. *Google Maps*. https://www.maps.google.com (accessed 2021-04-26).
(37) Kwon, H.-S.; Ryu, M. H.; Carlsten, C. Ultrafine Particles: Unique Physicochemical Properties Relevant to Health and Disease. *Exp. Mol. Med.* **2020**, *52*, 318−328.
(38) R Core Team. *R-A Language and Environment for Statistical Computing*. https://www.R-project.org (accessed Aug 18, 2021).
(39) PSCAA. *Air Quality Data. Puget Sound Clean Air Agency (PSCAA)*. https://pscleanair.gov/154/Air-Quality-Data (accessed April 06, 2020).
(40) Keller, J. P.; Olives, C.; Kim, S. Y.; Sheppard, L.; Sampson, P. D.; Szpiro, A. A.; Oron, A. P.; Lindström, J.; Vedal, S.; Kaufman, J. D. A Unified Spatiotemporal Modeling Approach for Predicting Concentrations of Multiple Air Pollutants in the Multi-Ethnic Study of Atherosclerosis and Air Pollution. *Environ. Health Perspect.* **2015**, *123*, 301−309.
(41) Young, M. T.; Bechle, M. J.; Sampson, P. D.; Szpiro, A. A.; Marshall, J. D.; Sheppard, L.; Kaufman, J. D. Satellite-Based NO2 and Model Validation in a National Prediction Model Based on Universal Kriging and Land-Use Regression. *Environ. Sci. Technol.* **2016**, *50*, 3686−3694.
(42) Pebesma, E.; Graeler, B. *Gstat: Spatial and Spatio-Temporal Geostatistical Modelling, Prediction and Simulation* 2021.
(43) R Core Team. *R: A Language and Environment for Statistical Computing*. R Foundation for Statistical Computing. https://www.r-project.org.
(44) Bi, J.; Carmona, N.; Blanco, M. N.; Gassett, A. J.; Seto, E.; Szpiro, A. A.; Larson, T. V.; Sampson, P. D.; Kaufman, J. D.; Sheppard, L. Publicly Available Low-Cost Sensor Measurements for PM2.5 Exposure Modeling: Guidance for Monitor Deployment and Data Selection. *Environ. Int.* **2022**, *158*, No. 106897.
(45) Roberts, D. R.; Bahn, V.; Ciuti, S.; Boyce, M. S.; Elith, J.; Guillera-Arroita, G.; Hauenstein, S.; Lahoz-Monfort, J. J.; Schröder, B.; Thuiller, W.; Warton, D. I.; Wintle, B. A.; Hartig, F.; Dormann, C. F. Cross-Validation Strategies for Data with Temporal, Spatial, Hierarchical, or Phylogenetic Structure. *Ecography* **2017**, *40*, 913−929.
(46) Kerckhoffs, J.; Hoek, G.; Portengen, L.; Brunekreef, B.; Vermeulen, R. C. H. Performance of Prediction Algorithms for Modeling Outdoor Air Pollution Spatial Surfaces. *Environ. Sci. Technol.* **2019**, *53*, 1413−1421.
(47) Kerckhoffs, J.; Hoek, G.; Gehring, U.; Vermeulen, R. Modelling Nationwide Spatial Variation of Ultrafine Particles Based on Mobile Monitoring. *Environ. Int.* **2021**, *154*, No. 106569.
(48) Minet, L.; Liu, R.; Valois, M. F.; Xu, J.; Weichenthal, S.; Hatzopoulou, M. Development and Comparison of Air Pollution Exposure Surfaces Derived from On-Road Mobile Monitoring and Short-Term Stationary Sidewalk Measurements. *Environ. Sci. Technol.* **2018**, *52*, 3512−3519.
(49) Simon, M. C.; Hudda, N.; Naumova, E. N.; Levy, J. I.; Brugge, D.; Durant, J. L. Comparisons of Traffic-Related Ultrafine Particle Number Concentrations Measured in Two Urban Areas by Central, Residential, and Mobile Monitoring. *Atmos. Environ.* **2017**, *169*, 113−127.
(50) Saha, P. K.; Li, H. Z.; Apte, J. S.; Robinson, A. L.; Presto, A. A. Urban Ultrafine Particle Exposure Assessment with Land-Use Regression: Influence of Sampling Strategy. *Environ. Sci. Technol.* **2019**, *53*, 7326−7336.
(51) Levy, I.; Mihele, C.; Lu, G.; Narayan, J.; Brook, J. R. Evaluating Multipollutant Exposure and Urban Air Quality: Pollutant Interrelationships, Neighborhood Variability, and Nitrogen Dioxide as a Proxy Pollutant. *Environ. Health Perspect.* **2014**, *122*, 65−72.
(52) Levy, I.; Mihele, C.; Lu, G.; Narayan, J.; Hilker, N.; Brook, J. R. Elucidating Multipollutant Exposure across a Complex Metropolitan Area by Systematic Deployment of a Mobile Laboratory. *Atmos. Chem. Phys.* **2014**, *14*, 7173−7193.
(53) US EPA. *NAAQS Table*. United States Environmental Protection Agency (US EPA). https://www.epa.gov/criteria-air-pollutants/naaqs-table (accessed July 07, 2021).
(54) Abernethy, R. C.; Allen, R. W.; McKendry, I. G.; Brauer, M. A Land Use Regression Model for Ultrafine Particles in Vancouver, Canada. *Environ. Sci. Technol.* **2013**, *47*, 5217−5225.
(55) Farrell, W.; Weichenthal, S.; Goldberg, M.; Valois, M.-F.; Shekarrizfard, M.; Hatzopoulou, M. Near Roadway Air Pollution across a Spatially Extensive Road and Cycling Network. *Environ. Pollut.* **2016**, *212*, 498−507.
(56) Hankey, S.; Marshall, J. D. On-Bicycle Exposure to Particulate Air Pollution: Particle Number, Black Carbon, PM2.5, and Particle Size. *Atmos. Environ.* **2015**, *122*, 65−73.
(57) Kerckhoffs, J.; Hoek, G.; Vlaanderen, J.; van Nunen, E.; Messier, K.; Brunekreef, B.; Gulliver, J.; Vermeulen, R. Robustness of Intra Urban Land-Use Regression Models for Ultrafine Particles and Black Carbon Based on Mobile Monitoring. *Environ. Res.* **2017**, *159*, 500−508.
(58) Montagne, D. R.; Hoek, G.; Klompmaker, J. O.; Wang, M.; Meliefste, K.; Brunekreef, B. Land Use Regression Models for Ultrafine Particles and Black Carbon Based on Short-Term

Monitoring Predict Past Spatial Variation. *Environ. Sci. Technol.* **2015**, *49*, 8712−8720.
(59) Patton, A. P.; Zamore, W.; Naumova, E. N.; Levy, J. I.; Brugge, D.; Durant, J. L. Transferability and Generalizability of Regression Models of Ultrafine Particles in Urban Neighborhoods in the Boston Area. *Environ. Sci. Technol.* **2015**, *49*, 6051−6060.
(60) Ragettli, M. S.; Ducret-Stich, R. E.; Foraster, M.; Morelli, X.; Aguilera, I.; Basagaña, X.; Corradi, E.; Ineichen, A.; Tsai, M. Y.; Probst-Hensch, N.; Rivera, M.; Slama, R.; Künzli, N.; Phuleria, H. C. Spatio-Temporal Variation of Urban Ultrafine Particle Number Concentrations. *Atmos. Environ.* **2014**, *96*, 275−283.
(61) Rivera, M.; Basagaña, X.; Aguilera, I.; Agis, D.; Bouso, L.; Foraster, M.; Medina-Ramón, M.; Pey, J.; Künzli, N.; Hoek, G. Spatial Distribution of Ultrafine Particles in Urban Settings: A Land Use Regression Model. *Atmos. Environ.* **2012**, *54*, 657−666.
(62) Saha, P. K.; Zimmerman, N.; Malings, C.; Hauryliuk, A.; Li, Z.; Snell, L.; Subramanian, R.; Lipsky, E.; Apte, J. S.; Robinson, A. L.; Presto, A. A. Quantifying High-Resolution Spatial Variations and Local Source Impacts of Urban Ultrafine Particle Concentrations. *Sci. Total Environ.* **2019**, *655*, 473−481.
(63) Saraswat, A.; Apte, J. S.; Kandlikar, M.; Brauer, M.; Henderson, S. B.; Marshall, J. D. Spatiotemporal Land Use Regression Models of Fine, Ultrafine, and Black Carbon Particulate Matter in New Delhi, India. *Environ. Sci. Technol.* **2013**, *47*, 12903−12911.
(64) van Nunen, E.; Vermeulen, R.; Tsai, M.-Y.; Probst-Hensch, N.; Ineichen, A.; Davey, M.; Imboden, M.; Ducret-Stich, R.; Naccarati, A.; Raffaele, D.; et al. Land Use Regression Models for Ultrafine Particles in Six European Areas. *Environ. Sci. Technol.* **2017**, *51*, 3336−3345.
(65) Weichenthal, S.; Van Ryswyk, K.; Goldstein, A.; Bagg, S.; Shekkarizfard, M.; Hatzopoulou, M. A Land Use Regression Model for Ambient Ultrafine Particles in Montreal, Canada: A Comparison of Linear Regression and a Machine Learning Approach. *Environ. Res.* **2016**, *146*, 65−72.
(66) Weichenthal, S.; Van Ryswyk, K.; Goldstein, A.; Shekarrizfard, M.; Hatzopoulou, M. Characterizing the Spatial Distribution of Ambient Ultrafine Particles in Toronto, Canada: A Land Use Regression Model. *Environ. Pollut.* **2016**, *208*, 241−248.
(67) Yu, C. H.; Fan, Z.; Lioy, P. J.; Baptista, A.; Greenberg, M.; Laumbach, R. J. A Novel Mobile Monitoring Approach to Characterize Spatial and Temporal Variation in Traffic-Related Air Pollutants in an Urban Community. *Atmos. Environ.* **2016**, *141*, 161−173.
(68) Beelen, R.; Hoek, G.; Fischer, P.; van den Brandt, P. A.; Brunekreef, B. Estimated Long-Term Outdoor Air Pollution Concentrations in a Cohort Study. *Atmos. Environ.* **2007**, *41*, 1343−1358.
(69) Brauer, M.; Hoek, G.; Vliet, P.; van Meliefste, K.; Fischer, P.; Gehring, U.; Heinrich, J.; Cyrys, J.; Bellander, T.; Lewne, M.; Brunekreef, B. Estimating Long-Term Average Particulate Air Pollution Concentrations: Application of Traffic Indicators and Geographic Information Systems. *Epidemiology* **2003**, *14*, 228−239.
(70) Carr, D.; von Ehrenstein, O.; Weiland, S.; Wagner, C.; Wellie, O.; Nicolai, T.; von Mutius, E. Modeling Annual Benzene, Toluene, NO2, and Soot Concentrations on the Basis of Road Traffic Characteristics. *Environ. Res.* **2002**, *90*, 111−118.
(71) Dodson, R. E.; Houseman, E. A.; Morin, B.; Levy, J. I. An Analysis of Continuous Black Carbon Concentrations in Proximity to an Airport and Major Roadways. *Atmos. Environ.* **2009**, *43*, 3764−3773.
(72) Hankey, S.; Marshall, J. D. Land Use Regression Models of On-Road Particulate Air Pollution (Particle Number, Black Carbon, PM2.5, Particle Size) Using Mobile Monitoring. *Environ. Sci. Technol.* **2015**, *49*, 9194−9202.
(73) Henderson, S. B.; Beckerman, B.; Jerrett, M.; Brauer, M. Application of Land Use Regression to Estimate Long-Term Concentrations of Traffic-Related Nitrogen Oxides and Fine Particulate Matter. *Environ. Sci. Technol.* **2007**, *41*, 2422−2428.
(74) Hochadel, M.; Heinrich, J.; Gehring, U.; Morgenstern, V.; Kuhlbusch, T.; Link, E.; Wichmann, H.-E.; Krämer, U. Predicting Long-Term Average Concentrations of Traffic-Related Air Pollutants Using GIS-Based Information. *Atmos. Environ.* **2006**, *40*, 542−553.
(75) Larson, T.; Su, J.; Baribeau, A.-M.; Buzzelli, M.; Setton, E.; Brauer, M. A Spatial Model of Urban Winter Woodsmoke Concentrations. *Environ. Sci. Technol.* **2007**, *41*, 2429−2436.
(76) Larson, T.; Henderson, S. B.; Brauer, M. Mobile Monitoring of Particle Light Absorption Coefficient in an Urban Area as a Basis for Land Use Regression. *Environ. Sci. Technol.* **2009**, *43*, 4672−4678.
(77) Morgenstern, V.; Zutavern, A.; Cyrys, J.; Brockow, I.; Gehring, U.; Koletzko, S.; Bauer, C. P.; Reinhardt, D.; Wichmann, H.-E.; Heinrich, J. Respiratory Health and Individual Estimated Exposure to Traffic-Related Air Pollutants in a Cohort of Young Children. *Occup. Environ. Med.* **2006**, *64*, 8−16.
(78) Ryan, P. H.; LeMasters, G. K.; Biswas, P.; Levin, L.; Hu, S.; Lindsey, M.; Bernstein, D. I.; Lockey, J.; Villareal, M.; Hershey, G. K. K.; Grinshpun, S. A. A Comparison of Proximity and Land Use Regression Traffic Exposure Models and Wheezing in Infants. *Environ. Health Perspect.* **2007**, *115*, 278−284.
(79) Su, J. G.; Allen, G.; Miller, P. J.; Brauer, M. Spatial Modeling of Residential Woodsmoke across a Non-Urban Upstate New York Region. *Air Qual. Atmos. Health* **2013**, *6*, 85−94.
(80) NOAA. *NOAA Climate.gov*. National Oceanic and Atmospheric Administration (NOAA). https://www.climate.gov (accessed July 07, 2021).
(81) Moran, D.; Kanemoto, K.; Jiborn, M.; Wood, R.; Többen, J.; Seto, K. C. Carbon Footprints of 13 000 Cities. *Environ. Res. Lett.* **2018**, *13*, No. 064041.
(82) Moran, D.; Kanemoto, K.; Wood, R.; Tobben, J.; Seto, K. *Global Gridded Model of Carbon Footprints (GGMCF)*. http://citycarbonfootprints.info (accessed July 07, 2021).
(83) Hoek, G.; Beelen, R.; de Hoogh, K.; Vienneau, D.; Gulliver, J.; Fischer, P.; Briggs, D. A Review of Land-Use Regression Models to Assess Spatial Variation of Outdoor Air Pollution. *Atmos. Environ.* **2008**, *42*, 7561−7578.
(84) Billionnet, C.; Sherrill, D.; Annesi-Maesano, I. Estimating the Health Effects of Exposure to Multi-Pollutant Mixture. *Ann. Epidemiol.* **2012**, *22*, 126−141.
(85) Dominici, F.; Peng, R. D.; Barr, C. D.; Bell, M. L. Protecting Human Health from Air Pollution: Shifting from a Single-Pollutant to a Multipollutant Approach. *Epidemiol. Camb. Mass* **2010**, *21*, 187−194.
(86) Oakes, M.; Baxter, L.; Long, T. C. Evaluating the Application of Multipollutant Exposure Metrics in Air Pollution Health Studies. *Environ. Int.* **2014**, *69*, 90−99.
(87) Stafoggia, M.; Breitner, S.; Hampel, R.; Basagaña, X. Statistical Approaches to Address Multi-Pollutant Mixtures and Multiple Exposures: The State of the Science. *Curr. Environ. Health Rep.* **2017**, *4*, 481−490.
(88) US EPA. *Integrated science assessment (ISA) for particulate matter*. US Environmental Protection Agency. https://cfpub.epa.gov/ncea/isa/recordisplay.cfm?deid=347534 (accessed April 06, 2021).
(89) Saha, P. K.; Li, H. Z.; Apte, J. S.; Robinson, A. L.; Presto, A. A. Urban Ultrafine Particle Exposure Assessment with Land-Use Regression: Influence of Sampling Strategy. *Environ. Sci. Technol.* **2019**, *53*, 7326−7336.
(90) Sabaliauskas, K.; Jeong, C. H.; Yao, X.; Reali, C.; Sun, T.; Evans, G. J. Development of a Land-Use Regression Model for Ultrafine Particles in Toronto, Canada. *Atmos. Environ.* **2015**, *110*, 84−92.
(91) Beelen, R.; Hoek, G.; Vienneau, D.; Eeftens, M.; Dimakopoulou, K.; Pedeli, X.; Tsai, M.-Y.; Künzli, N.; Schikowski, T.; Marcon, A.; Eriksen, K. T.; Raaschou-Nielsen, O.; Stephanou, E.; Patelarou, E.; Lanki, T.; Yli-Tuomi, T.; Declercq, C.; Falq, G.; Stempfelet, M.; Birk, M.; Cyrys, J.; von Klot, S.; Nádor, G.; Varró, M. J.; Dėdelė, A.; Gražulevičienė, R.; Mölter, A.; Lindley, S.; Madsen, C.; Cesaroni, G.; Ranzi, A.; Badaloni, C.; Hoffmann, B.; Nonnemacher, M.; Krämer, U.; Kuhlbusch, T.; Cirach, M.; de Nazelle, A.; Nieuwenhuijsen, M.; Bellander, T.; Korek, M.; Olsson, D.; Strömgren, M.; Dons, E.; Jerrett, M.; Fischer, P.; Wang, M.;

Brunekreef, B.; de Hoogh, K. Development of NO2 and NOx Land Use Regression Models for Estimating Air Pollution Exposure in 36 Study Areas in Europe − The ESCAPE Project. *Atmos. Environ.* **2013**, *72*, 10−23.
(92) Wolf, K.; Cyrys, J.; Harciníková, T.; Gu, J.; Kusch, T.; Hampel, R.; Schneider, A.; Peters, A. Land Use Regression Modeling of Ultrafine Particles, Ozone, Nitrogen Oxides and Markers of Particulate Matter Pollution in Augsburg, Germany. *Sci. Total Environ.* **2017**, *579*, 1531−1540.
(93) Cattani, G.; Gaeta, A.; Di Menno di Bucchianico, A.; De Santis, A.; Gaddi, R.; Cusano, M.; Ancona, C.; Badaloni, C.; Forastiere, F.; Gariazzo, C.; Sozzi, R.; Inglessis, M.; Silibello, C.; Salvatori, E.; Manes, F.; Cesaroni, G. Development of Land-Use Regression Models for Exposure Assessment to Ultrafine Particles in Rome, Italy. *Atmos. Environ.* **2017**, *156*, 52−60.
(94) Hoek, G.; Beelen, R.; Kos, G.; Dijkema, M.; Zee, S. C.; van der Fischer, P. H.; Brunekreef, B. Land Use Regression Model for Ultrafine Particles in Amsterdam. *Environ. Sci. Technol.* **2011**, *45*, 622−628.
(95) Saha, P. K.; Hankey, S.; Marshall, J. D.; Robinson, A. L.; Presto, A. A. High-Spatial-Resolution Estimates of Ultrafine Particle Concentrations across the Continental United States. *Environ. Sci. Technol.* **2021**, *55*, 10320−10331.
(96) Eeftens, M.; Meier, R.; Schindler, C.; Aguilera, I.; Phuleria, H.; Ineichen, A.; Davey, M.; Ducret-Stich, R.; Keidel, D.; Probst-Hensch, N.; Künzli, N.; Tsai, M. Y. Development of Land Use Regression Models for Nitrogen Dioxide, Ultrafine Particles, Lung Deposited Surface Area, and Four Other Markers of Particulate Matter Pollution in the Swiss SAPALDIA Regions. *Environ. Health* **2016**, *15*, 1−14.
(97) Messier, K. P.; Chambliss, S. E.; Gani, S.; Alvarez, R.; Brauer, M.; Choi, J. J.; Hamburg, S. P.; Kerckhoffs, J.; Lafranchi, B.; Lunden, M. M.; Marshall, J. D.; Portier, C. J.; Roy, A.; Szpiro, A. A.; Vermeulen, R. C. H.; Apte, J. S. Mapping Air Pollution with Google Street View Cars: Efficient Approaches with Mobile Monitoring and Land Use Regression. *Environ. Sci. Technol.* **2018**, *52*, 12563−12572.

https://doi.org/10.1021/acs.est.2c01077
Environ. Sci. Technol. 2022, 56, 11460−11472